Large Core Optical Fibre Refractive Index Sensor

A Dissertation submitted towards the partial fulfillment of
the requirement for the award of degree of

Master of Technology

In

Microwave and Optical Communication Engineering

Submitted By

Himanshu Mohan
04/MOC/2010

Under the supervision of

Dr. Ajeet Kumar
(Assistant Professor)

Department of Electronics and Communication Engineering

&

Department of Applied Physics

Delhi Technological University

(Formerly Delhi College of Engineering)

CERTIFICATE

This is to certify that the dissertation title ***"Large Core Optical Fiber Refractive Index Sensor"*** is the authentic work of **Mr. Himanshu Mohan** under my guidance and supervision in the partial fulfillment of requirement towards the degree of Master of Technology in ***Microwave and Optical Communication Engineering***, jointly run by the Deptt.of Electronics and Communication Engineering and Deptt.of Applied Physics in ***Delhi Technological University.***

Dr. Ajeet Kumar	Prof. Rajiv Kapoor
Supervisor	HOD
Assistant Professor	Deptt. of ECE
Delhi Technological University	Delhi Technological University

ACKNOWLEDGEMENT

I am indebted to my thesis supervisor **Dr. Ajeet Kumar**, Department of Physics, for his gracious encouragement and very valued constructive criticism that has driven me to carry the project successfully.

I am deeply grateful to **Prof. Rajiv Kapoor**, Head of Department (Electronics and Communication Engineering), Delhi Technological University for his support and encouragement in carrying out this project.

I wish to express my heart full thanks to my branch coordinator **Prof. R.K Sinha & Dr. Priyanka Jain** and friends for their goodwill and support that helped me a lot in successful completion of this project.

I express my deep sense of gratitude to my mother **Dr. Gomti Dwivedi** and my friend **Sunny** for their time to time supports and encouragements.

Finally I would like to thank **Lord Krishna** for his blessings without which nothing is possible in this world.

Himanshu Mohan

M.Tech (MOCE)

04/MOC/2010

Table of Contents

List of Figures

ABSTRACT

Different chemical substances as well as several physical and biological parameters can be detected through measurements of the refractive index (RI). For this reason, RI sensors have gained considerable attention by the sensor community. Fiber-based refractometric devices are attractive, owing to the inherent advantages over their counterparts based on other techniques. For example, they can be multiplexed on a single fiber network and are suitable for *in situ* and remote RI measurements. Moreover, they are compact and lightweight.

In addition, the amount of sample needed to carry out the measurements can be very small. The resolution of fiber-based RI sensors can be as high as 10^{-5}. So far, different alternatives have been proposed to design RI sensors with conventional optical fibers. These include core-exposed or tapered fibers , fiber Bragg gratings (FBGs) , long period gratings (LPGs) , interferometers made with FBGs or LPGs, Refractive index sensors based on core diameter mismatch etc. The advent of micro structured optical fibers has also opened new possibilities for RI sensing.

Chapter 1

Introduction

1.1 Optical Fiber for Communications

Fiber-optic communication [1, 2, 3] is a method of transmitting information from one place to another by sending pulses of light through an optical fiber. The light forms an electromagnetic carrier wave that is modulated to carry information. First developed in the 1970s, fiber-optic communication systems have revolutionized the telecommunications industry and have played a major role in the advent of the Information Age. Because of its advantages over electrical transmission, optical fibers have largely replaced copper wire communications in core networks in the developed world.

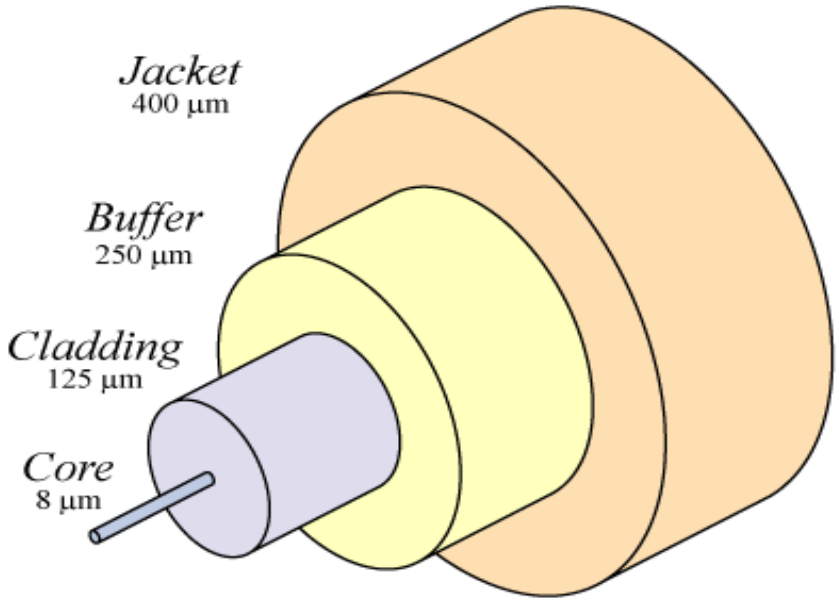

Figure. 1.1 *Schematic of a simple optical fiber*

1.2 Process of Communication

The process of communicating using fiber-optics [3] involves the following basic steps: Creating the optical signal involving the use of a transmitter, relaying the signal along the fiber, ensuring that the signal does not become too distorted or weak, receiving the optical signal, and converting it into an electrical signal. The following figure shows the key sections of an optical fiber communications link, which are as follows:

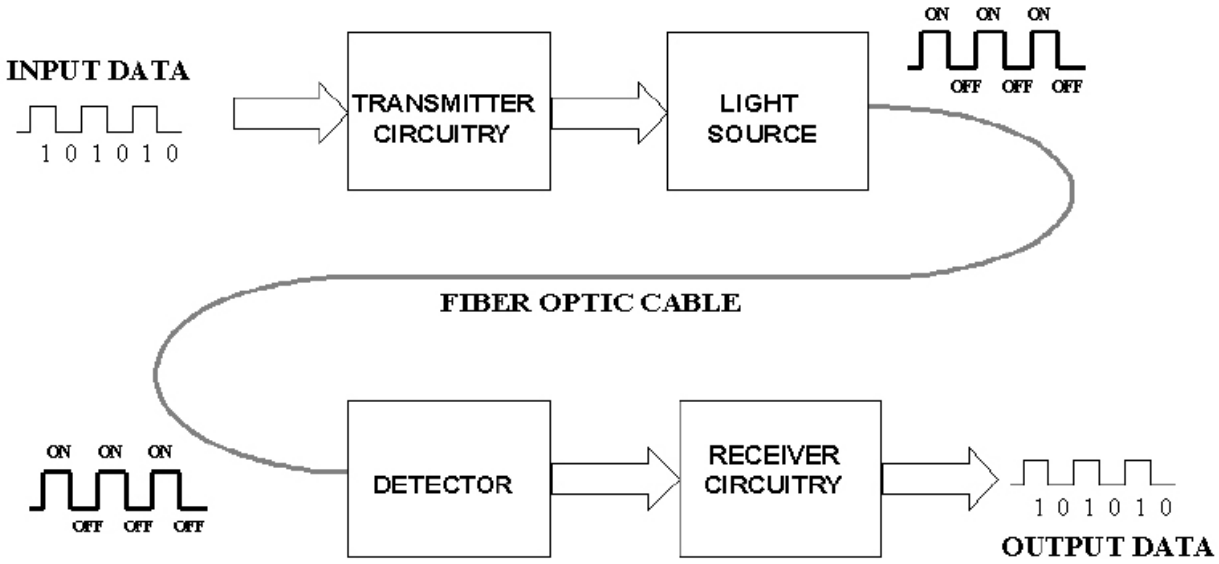

Figure 1.2 Simple optical fiber communication system

1.3 Other Applications of Optical Fiber

Optical Fibers can also be used in many other applications like,

1. Illumination Applications
2. Imaging Optics (In Medical Industry)
3. Spectroscopy
4. As a gain medium of a Laser
5. As a Fiber Optic Sensors

1.4 Fiber Optic Sensors

Optical fibers can be used as sensors [1,2] to measure Refractive Index, strain, temperature, pressure and other quantities by modifying a fiber so that the property to measure modulates the power transferred, intensity, phase, polarization, wavelength, or transit time of light in the fiber. Sensors that vary the intensity of light are the simplest, since only a simple source and detector are required. A particularly useful feature of such fiber optic sensors is that they can, if required, provide distributed sensing over distances of up to one meter.

1.5 Refractive Index Sensor

Different chemical substances as well as several physical and biological parameters can be detected through measurements of the refractive index (RI). For this reason, RI sensors [7, 9, 14] have gained considerable attention by the sensor community. Fiber-based refractometric devices [5] are attractive, owing to the inherent advantages over their counterparts based on other techniques. For example, they can be multiplexed on a single fiber network and are suitable for *in situ* and remote RI measurements. Moreover, they are compact and lightweight. In addition, the amount of sample needed to carry out the measurements can be very small. The resolution of fiber-based RI sensors can be as high as 10^{-5}. So far, different alternatives have been proposed to design RI sensors with conventional optical fibers. These include core-exposed or tapered fibers, fiber Bragg gratings (FBGs) [6], long period gratings (LPGs) [9, 11] interferometers made with FBGs or LPGs, Refractive index sensors based on core diameter mismatch etc. The advent of micro structured optical fibers has also opened new possibilities for RI sensing.

1.6 Objectives and Organization of the Thesis

This thesis is concerned with the design of Large Core Optical Fiber Refractive index Sensor [7], with a core diameter mismatch which is very much a topical area of research. Prior to this a single mode core diameter mismatch refractive index sensor has been developed in which the sensing region has been achieved by etching out the whole cladding and some portion of the core of the fiber. If sensing region is placed in different refractive

index medium then the cladding, the modal field distribution changes. The overlap of modal fields in the cladded region and the sensing region gives an estimate of fractional power transfer from the input end to output end. This fractional power transfer gives us the refractive index of the medium.

So the objective of this thesis is to design and analyze the Refractive Index sensor having the discontinuity between sensing region and cladding area by large core diameter.

The thesis consists of five chapters. Each chapter has its own introduction. This dissertation has been ordered in such a way that the process of constructing the proposed Large Core Optical Fiber Refractive Index sensor is evident throughout.

Proceeding in a logical manner, **Chapter 2** introduces the Specialty fibers.

Chapter 3 focus is placed on the Method of Analysis which includes Transfer Matrix Method [12, 18] and Transfer of power Method which is a powerful tool for the analysis of Refractive Index Sensors.

Chapter 4 presents the design and analysis of proposed novel design for refractive index sensing.

Chapter 5 Finally, the conclusion and scope for the future work are given in this chapter.

Chapter 2

Specialty Optical Fiber

The introduction of wavelength division multiplexing (WDM) technology put even greater demands on fiber design and composition to achieve wider bandwidth and flat gain. Efforts to extend the bandwidth of erbium doped fibers and develop amplifiers at other wavelength such as 1300 nm have spurred development of other dopants. Doping with ytterbium (Yb) allows pumping from 900 to 1090 nm using solid-state lasers or Nd and Yb fiber lasers. Of recent interest is the ability to pump Er/Yb fibers in a double-clad geometry with high power sources at 920 or 975 nm. Double-clad fibers are also being used to produce fiber lasers using Yb and Nd. Besides the amplification fiber, the erbium-doped amplifier requires a number of optical components for its operation. These include wavelength multiplexing and polarization multiplexing devices for the pump and signal wavelengths. Filters for gain flattening, power attenuators, and taps for power monitoring among other optical components are required for module performance. Also, because the amplifier-enabled transmission distances of hundreds of kilometers without regeneration, other propagation properties became important. These properties include chromatic dispersion, polarization dispersion, and nonlinearities such as four-wave mixing (FWM), self- and cross-phase modulation, and Raman and Brillouin scattering. Dispersion compensating fibers were introduced in order to deal with wavelength dispersion. Broadband compensation was possible with specially designed fibers. However, coupling losses between the transmission and the compensating fibers was an issue. Specially designed mode conversion or bridge fibers enabled low-loss splicing among these three fibers, making low insertion loss dispersion compensators possible. Fiber components as well as micro optic or in some instances planar optical components can be fabricated to provide for these applications. Generally speaking, but not always, fiber components enable the lowest insertion loss per device. A number of these fiber devices can be fabricated using standard SMF, but often special fibers are required. Specialty fibers are designed by changing fiber glass composition, refractive index profile, or coating to achieve certain unique properties

and functionalities. In addition to applications in optical communications, specialty fibers find a wide range of applications in other fields, such as industrial sensors, biomedical power delivery and imaging systems, military fiber gyroscope, high power lasers. A Few such fibers are described in the following.

2.1. Bragg Fibers

Bragg fibers [20] were proposed theoretically as early as in 1978, but only recently have such structures been demonstrated. Since then, they have attracted much attention, mainly because they offer the possibility of air guiding. Some important advantages of air core fibers are the possibility of reducing propagation loss below the level of 0.2 dB/km (the value of current telecommunication fibers), and the greatly increased power threshold for the onset of nonlinear optical phenomena such as stimulated Raman scattering. The air core fibers in the literature can be roughly classified in two categories, (i) Bragg fibers, where the air core is surrounded by cylindrical dielectric layers with alternating refractive indices, and (ii) photonic crystal fibers (PCF) [16], where the fiber cladding is composed of a two dimensional (2D) array of air holes. PCFs are typically based on silica glass, which has excellent material properties and forms the backbone of modern optical telecommunications, whereas current air core Bragg fibers are based on a combination of polymer and soft glass.

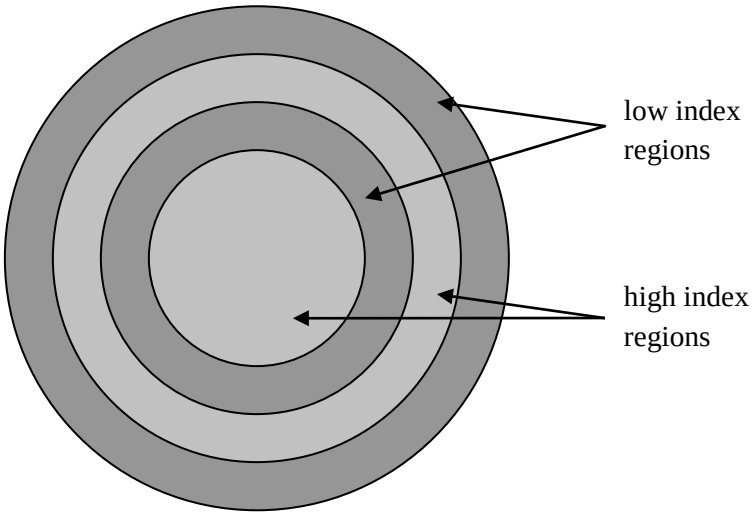

Figure. 2.1. Schematic diagram of a Bragg fiber

Fiber Bragg gratings (FBGs) [6] are spectral filters fabricated within segments of optical fiber. They typically reflect light over a narrow wavelength range and transmit all other wavelengths, but they also can be designed to have more complex spectral responses. Many uses exist for FBGs in today's fiber communications systems, which rely heavily on dense wavelength division multiplexing (WDM), and optical amplification.

FBGs are based on the principle of Bragg reflection. When light propagates through periodically alternating regions of higher and lower refractive index, it is partially reflected at each interface between those regions. If the spacing between those regions is such that all the partial reflections add up in phase i.e. when the round trip of the light between two reflections is an integral number of wavelengths, the total reflection can grow to nearly 100%, even if the individual reflections are very small. Of course, that condition will only hold for specific wavelengths. For all other wavelengths, the out of phase reflections end up canceling each other, resulting in high transmission.

To create the appropriate stack of high and low-refractive-index regions along a piece of optical fiber, manufacturers must permanently modify the refractive index of the fiber via the photosensitive effect. This is accomplished by exposing the optical fiber to ultraviolet (UV) light with a wavelength around 240 nm or less. The photosensitivity is primarily due to the germanium dopant used in the core of most commercial fibers. Photosensitivity can be increased by raising the germanium doping level, or by in-diffusing molecular hydrogen, which acts as a catalyst to the reaction of the germanium with UV light and greatly reduces exposure time. The index change is very stable, even at high temperatures, especially if the grating is preannealed (heated to a temperature between 150°C and 500°C after fabrication). The fabrication itself is a simple four step process: Remove the acrylate coating, expose the fiber to UV light, preanneal, and then recoat the fiber. To create a Bragg grating in an optical fiber, one needs to generate the required periodic pattern of UV light on the side of the fiber. This can be done by splitting a UV laser beam and recombining it in the fiber to form a standing wave, the period of which depends on the angle between the beams. Through the photo- sensitive effect, that pattern is imprinted into the fiber as a periodically varying change in refractive index. Changing the period merely requires changing the angle of the mirrors.

Early demonstrations of FBG fabrication used such an interferometric approach, but the stability of the interference pattern could easily be compromised by mechanical vibrations. A more reliable method for volume manufacturing uses phase masks to contact print the gratings. A phase mask is itself a grating, etched in silica that diffracts

UV light at normal incidence into the +1 and –1 diffractive orders. These two orders interfere to create the desired interference pattern just behind the mask, which is where the fiber is placed. Typical exposure times vary from a few seconds to a few minutes, depending on the type and strength of grating.

2.2. Photonic Crystal Fibers

A new class of optical fiber, called photonic crystal fiber (PCF) [26] has attracted considerable interest since their initial invention for their unusual optical properties. These fibers are characterized by microscopic air holes running along the fiber thorough the entire length of the fiber. These fibers are also known as mocrostructured fibers. Among the interesting novel features associated with these fibers are their endless single-mode operation from UV to IR spectral region , easy tolerance for dispersion and polarization control, possibility of obtaining large core single mode fiber and zero group velocity dispersion at short wavelength. These features mean that they are the subject of a growing research and development effort. The special index profile of microstructures fibers leads to exceptional guiding properties which cannot be obtained in the conventional step index fibers. The structure provides a wavelength dependent effective index for the cladding for which single mode guidance for a large range of wavelength becomes possible. There is a class of PCF in which the arrangement of air holes need not be regular and periodic fashion. These fibers are also referred to as holey fibers.

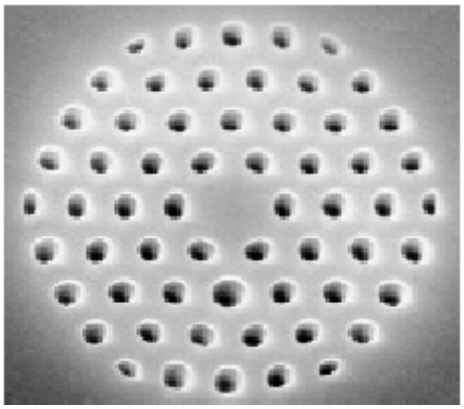

Figure. 2.2. Photonic crystal fiber cross section

The light guidance through the microstructured fibers can take place by two different mechanisms: average effective refractive index effect and photonic bandgap effect. For average refractive index model, the cladding full of air holes are replaced by a layer of average refractive index and the light guidance can be explained by simple and conventional principle of successive total internal reflection. For this model the array of air holes need not be regular, periodic, lattice-like structure. For the photonic bandgap mechanism of light guidance through a fiber, periodic arrangements of air holes are essential and these fibers are called photonic bandgap fibers. In these fibers the periodic arrangement of air holes in the cladding region of the fiber leads to the formation of photonic bandgap in the transverse plane of the fiber. Frequencies within this band gap cannot propagate in the cladding and are thus confined to propagate within the core which acts as a defect in the otherwise ‘perfect’ periodic structure.

In 1991, the idea emerged that light could be trapped inside a hollow fiber core by creating a periodic wavelength-scale lattice of microscopic holes in the cladding glass known as a photonic crystal. To understand how this might work, consider that all wavelength-scale periodic structures exhibit ranges of angle and color ("stop bands") where incident light is strongly reflected. This is the origin of the color in butterfly wings, peacock feathers, and holograms such as those found on credit cards. In photonic band gap (PBG) materials, however, these stop bands broaden to block propagation in every direction, resulting in the suppression of all optical vibrations within the range of wavelengths spanned by the photonic band gap. Appropriately designed, the holey photonic crystal cladding, running

along the entire length of the fiber, can prevent the escape of light from a hollow core. Thus, it becomes possible to escape the strait jacket of total internal reflection and trap light in a hollow fiber core surrounded by glass.

In the early 1970s, there had been the suggestion that a cylindrical Bragg waveguide might be produced in which rings of high and low refractive index are arranged around a central core. Recently, a successful solid-core version of this structure, made using modified chemical vapor deposition (MCVD), was reported. The effort is now heading toward a hollow core version, an ambitious goal that requires a materials system with much larger refractive index contrast than the few percent offered by MCVD [27] .

There are various applications of it. Among the more important ones, are rare-earth doped lasers and amplifiers and sensors. Also, the possibility of fashioning fibers from traditionally "difficult" materials such as infrared glasses opens up the prospect of a single-mode fiber that could transmit 10.6 μm light with low loss and at high powers; this would revolutionize the field of laser machining.

Photonic crystal fibers represent a next-generation, radically improved version of a well-established and highly successful technology. In escaping from the confines of conventional fiber optics, PCFs have created a renaissance of new possibilities in a large number of diverse areas of research and technology, in the process irrevocably breaking many of the tenets of received wisdom in fiber optics.

Through photonic band gap manipulation cladding material can be engineered that does not support any modes for certain frequencies, creating total internal reflection. The engineerable birefringence allows for relatively high refractive index contrasts. This allows a mode to be confined in a core much smaller than previously possible, less than the wavelength of the light. The current performance of single-mode optical fibers results from many years of intensive research. There appears to be no reason why the losses in Photonic Crystal Fibers cannot be reduced to or below that of standard optical fibers. Similar development effort could lead to explosive growth in photonic crystal fiber technology over the coming years.

2.3. Segmented Cladding Fibers

A new type of fiber, known as Segmented cladding fiber (SCF) were proposed [28] as an alternative to the holey fibers for the provision of single mode operation over an extended range of wavelengths. It was then shown that an SCF could be designed as an ultra large core single mode fiber for optical communication, which could suppress effectively the non-linear optical effects because of its large core size. It also provides a much higher transmission capacity because of its potentially weak birefringence, compared with a holey fiber.

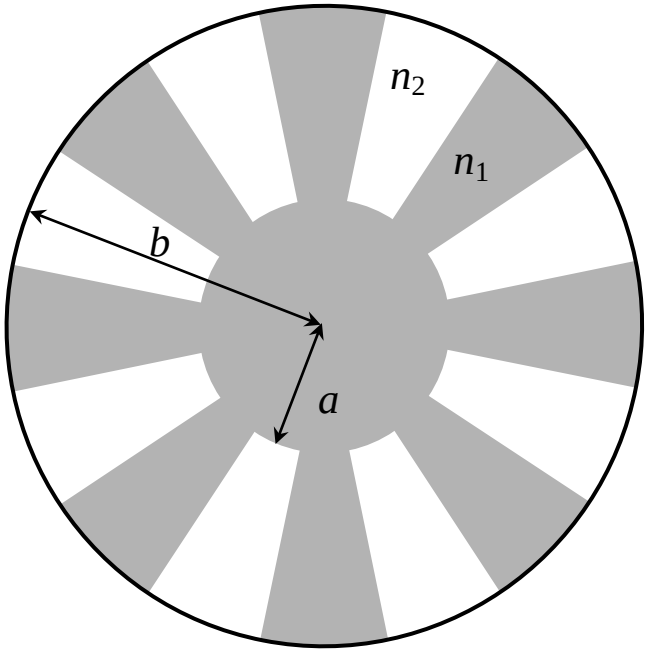

Figure. 2.3. Structure of a segmented cladding fiber

A SCF is characterized by the cladding with regions of high and low refractive index alternating regularly with uniform core of high refractive index. The SCF uses small index contrast unlike holey fiber and hence exhibits some better qualities over photonic crystal fibers. It has potentially low polarization mode dispersion which is essential for high bit rate transmission. The chromatic dispersion of SCF is also expected to be similar to that of conventional fiber so that it can be controlled by conventional techniques. An SCF can be bare segmented cladding fiber or coated segmented cladding fiber. For the former, the vsegmented cladding is surrounded by air and for the later, the segmented cladding of the

SCF extends to infinity. The effective index decreases monotonously towards the core index and eventually exceeds the mode index of the fundamental mode. An infinitely extended SCF is therefore a leaky structure and all the modes of the fiber suffer from leakage loss. In practice, the fiber is truncated a finite cladding radius and coated with a high index material. A high index surrounding is similar to that of an infinitely extended cladding and at the same time shields the fiber from external perturbations.

2.4. Large Mode Area Fibers

Multimode optical fiber cannot be used for long distance data transmission due to the intermodal dispersion. Fiber non-linear effects limit the bit transfer rate for single mode fiber because of its small core diameter. In recent years, large-mode-area-fibers have attracted our considerable interest because increased mode field area allows higher peak power within the core before non-linear effects become significant and operative. Longer amplifier spacing can also be used for higher effective area.

Single mode fiber with low dispersion slope and large core area is most desirable for long-haul terrestrial and submarine transmission system and high capacity DWDM system. But, large mode area allows a number of modes to propagate. In the case of conventional fibers, the effective area is limited by the fact that an increasing core size requires a correspondingly decreasing index step between the core and the cladding in order to maintain single-mode operation. This imposes requirements on the control of the index profile which is difficult to realize with doping of the glass.

Knight et al. [30] showed that ultra large core single mode fiber can be achieved from a holey fiber by suitably choosing the hole diameter and spacing. They have fabricated a holey fiber with a core diameter of 22.5 μm, the number of guide mode of this fiber does not depend on core radius and wavelength.

Mortensen et al. [29] worked on the photonic crystal fiber and found that enhancement of mode area by 30% can be achieved without a corresponding decrease in attenuation. They demonstrated that triangular distribution of air hole in the cladding and suitable chose of hole diameter can improve the mode area and the loss properties of holey fiber.

To date, most work in this area has concentrated on rare-earth-doped optical fiber with large mode area to improve their energy storage characteristics in compromise of gain efficiency. A number of erbium doped fiber with large mode area have been fabricated which demonstrated their effectiveness as optical amplifiers and in Q-switched fiber lasers. Shizhu Yin et al. [31] made a new design of fiber having large effective area over 100 μm^2 which can be used in DWDM system for its non-zero dispersion shifting characteristics. This fiber also showed low bending and splicing loss.

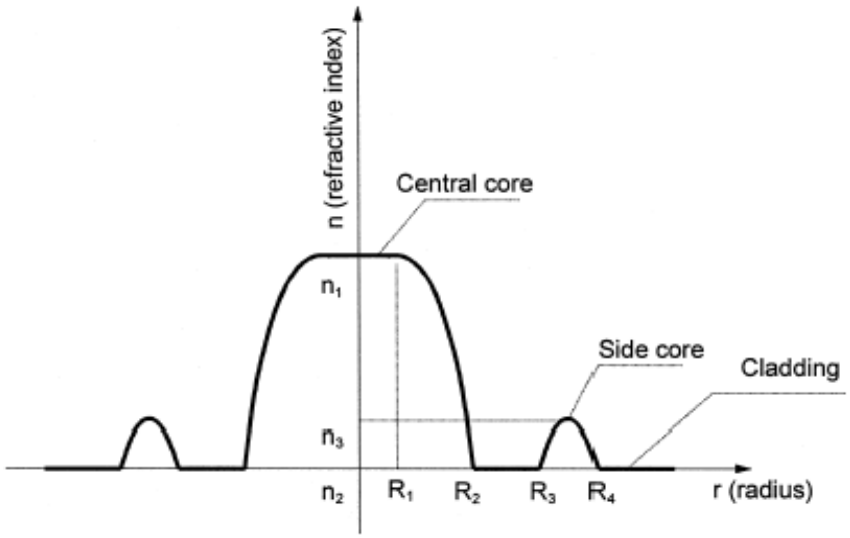

Figure. 2.4 Refractive index profile of a fiber designed by Shizhu Yin et al

2.5. Raised Inner Cladding Fibers

These fibers consist of five layers of which four layers form the cladding. The cladding layers have low and high indices alternatively.

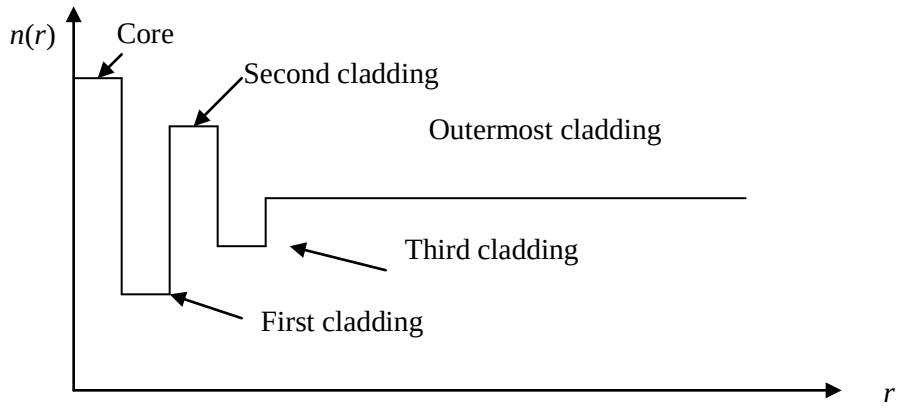

Figure.2.5. Refractive index profile of a typical raised inner cladding fiber

The objective of this structure has low loss and low dispersion at both the 1.3 μm and 1.55 μm wavelengths. This fiber shows uniform dispersion properties in this wavelength range.

2.6. Large Mode Area Multiclad Leaky Fiber

LMA multiclad leaky fibers are used in effective single mode operation by large differential leakage loss between the fundamental mode and higher order modes [12, 14, 21]. These designs include periodically arranged high and low refractive index segments in the angular direction of cladding [12, 21, 22] a graded index cladding with radially rising refractive index [13] and a cladding mode of periodically arranged low index trenches of varying strength in an otherwise high index medium [14].

2.7. Depressed Inner Cladding (DIC) Fibers

These fibers have two claddings and are also called double clad fibers. Each cladding has a refractive index that is lower than that of the core. Of the two claddings, inner and outer, the inner cladding has the lower refractive index. A doubly clad fiber has the advantage of very low macrobending losses. It also has two zero-dispersion points and low dispersion over a much wider wavelength range than a singly clad fiber [25].

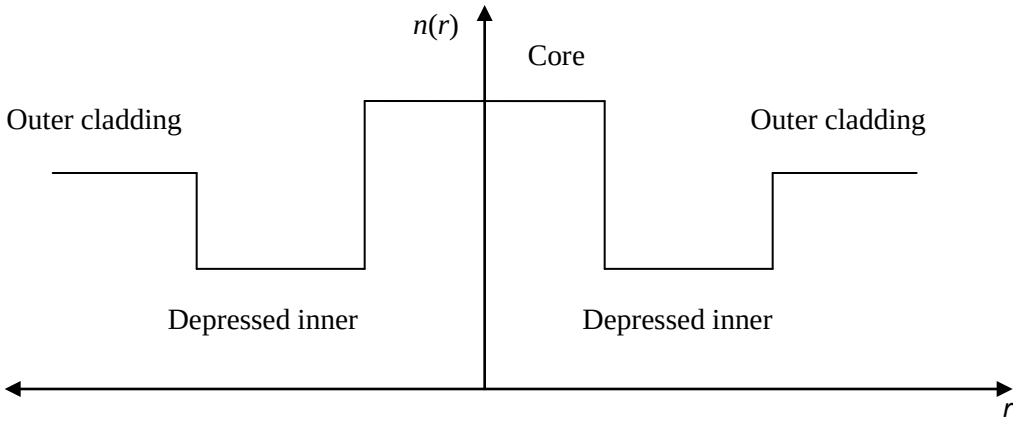

Fig 2.6 Refractive index profile of typical DIC fiber.

Chapter 3

Large Mode Area Refractive Index Sensor

Aim of this thesis is to present a large core single mode refractive index sensor. It is impossible to achieve single mode operation by a large core conventional fiber. So we have used a specialty fiber that is co-axial duel core leaky fiber [24]. The fiber works on the principle of mode filtering. By using the concept of core-diameter mismatch such a large core single mode fiber can be used to design a single single-mode refractive index sensor for wide refractive index.

3.1 Co-axial Duel Core Leaky Fiber

The refractive index profile of the proposed design is shown in the Fig. 3.1 and is defined as

$$n(\mathrm{r}) = \begin{cases} n_1; & 0 < r < a \\ n_2; & a < r < b \\ n_1; & b < r < c \\ n_3; & c < r < d \\ n_1; & r > d \end{cases} \qquad (3.1)$$

where $n_1 > n_3 > n_2$.

The high index regions $0 < r < a$ and $b < r < c$ define inner and outer cores of the fiber, respectively. The regions $a < r < b$ and $c < r < d$ are depressed cladding regions and can be defined as inner and outer cladding respectively. The outermost high index region ($r > d$) makes the overall design leaky, and all the modes suffer from finite leakage loss. The width of different layers are defined as $d_1 = b - a$, $d_2 = c - b$ and $d_3 = d - c$.

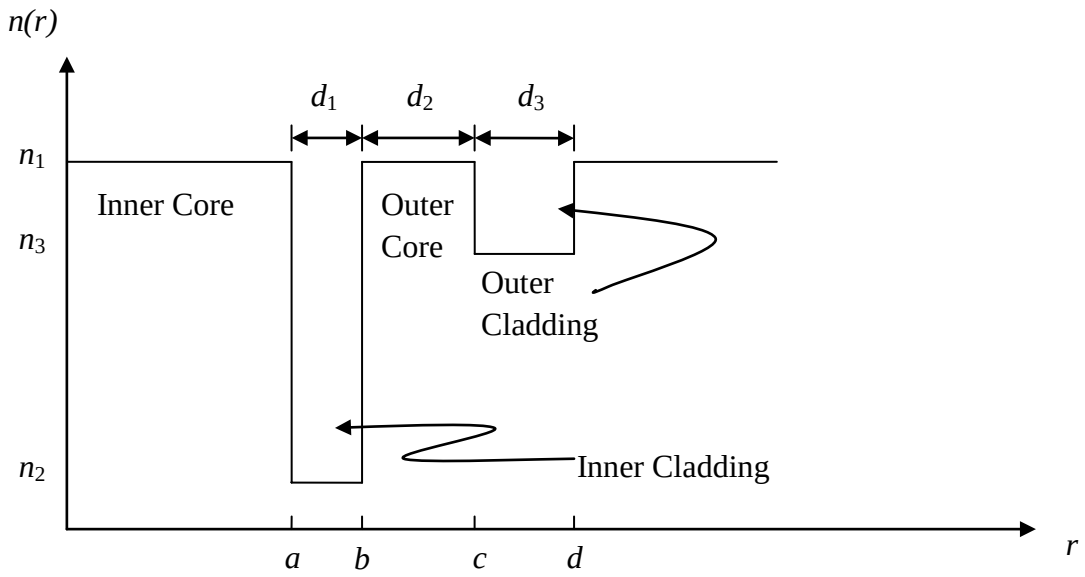

Figure 3.1 Schematic of the refractive index profile of a co-axial duel core leaky fiber

We have used the Transfer matrix method (TMM) [8] to calculate the leakage losses of the modes. The TMM is particularly useful for analyzing multi layer structures. In the TMM an arbitrary refractive index profile is divided into large number of homogeneous layers by using the staircase approximation.

3.2 Transfer Matrix Method

There has been considerable interest in developing accurate numerical approximate techniques to study the propagation characteristics of absorbing, non-absorbing or leaky planar waveguide structures. The use of the matrix method in studying the propagation of plane electromagnetic waves through a stratified medium is well known in optics. Since a planar waveguide is nothing more than a stack of thin films, the standard mathematical methods used in the analysis of optical coatings, such as interference filters can be extended to include optical waveguides. In essence this method involves determination of the transfer matrix of the system and then using the properties of a guided mode to obtain a characteristic equation. The solutions of this transcendental equation give the propagation constants of the modes of the waveguide. In general, the above method become tedious as

the number of films increases and, in particular, become complicated for analyzing absorbing/lossy structures as they involve the solution of complex transcendental equations. The transcendental equations can be solved very easily by matrix method which is used for the analysis of the proposed structure. The present fiber is analyzed by simple method involving multiplication of 2 × 2 matrices from which we can readily obtain the real and imaginary parts of the propagation constants as well as the field configurations for arbitrarily graded planar structures. We have applied the method to obtain leakage and absorption losses in planar waveguide structure. Since exact analysis for graded index optical fibers is difficult and time-consuming, appropriate approximation techniques have been developed. Among them, scalar approximation analysis is one of the most widely used techniques. The error due to the scalar approximation is thought to be sufficiently small for calculating impulse responses in multimode optical fibers.

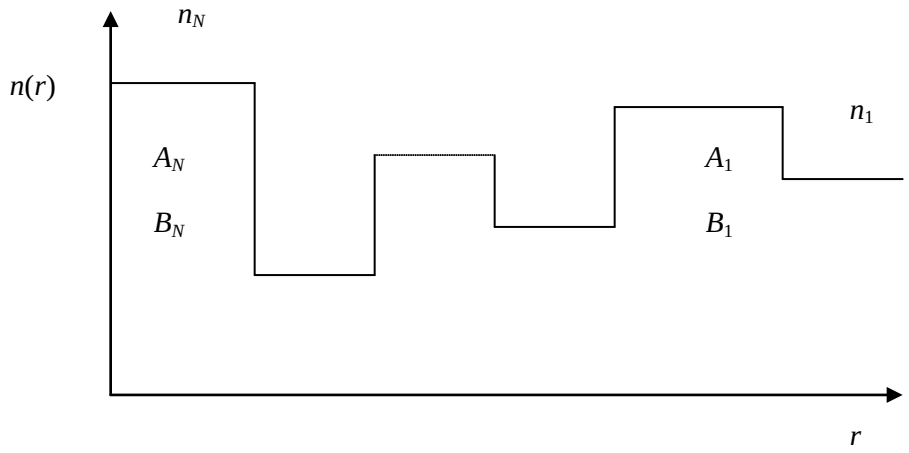

Figure 3.2 Refractive index profile of a radially symmetric optic fiber having multilayer structure

It is assumed that the permittivity of the fiber depends only on the distance r from the axis, and the permeability is equal to that of vacuum. We consider an optical fiber having a radially symmetric refractive index profile and consisting of N regions having refractive indices n_1, n_2, n_3, … n_N as shown in the above Fig. Under the scalar approximation, the equation describing the radial part of the modal field in the pth region is given by

$$r^2 \frac{d^2R}{dr^2} + r\frac{dR}{dr} + [(k_0{}^2 n_p{}^2 - \beta^2)r^2 - l^2]R = 0 \qquad (3.2)$$

We have assumed that the modal field will be given by

$$\psi(r,\phi,z,t) = R(r)\begin{bmatrix}\cos\phi l \\ \sin\phi l\end{bmatrix}\exp i(\omega t - \beta z) \qquad l = 1,2,3,\ldots..$$

$$r^2 \frac{d^2R}{dr^2} + r\frac{dR}{dr} + [(k_0{}^2 n_p{}^2 - \beta^2)r^2]R = 0 \qquad (3.3)$$

The solution for this equation can be given analytically by standard Bessel functions which describe the transverse field inside the fiber. In the attenuating region, where $\beta^2 < k_0{}^2 n_p{}^2$ the general solution of equation (2) is given by:

$$R(r) = A_p J_0(k_p r) + B_p Y_0(k_p r) \qquad (3.4)$$

And in the guiding region, where $\beta^2 > k_0{}^2 n_q{}^2$

$$R(r) = A_q K_0(\gamma_q r) + B_q I_0(\gamma_q r) \qquad (3.5)$$

$$\text{Where } k_p{}^2 = k_0 n_p{}^2 - \beta^2; \qquad \gamma_q{}^2 = \beta^2 - k_0{}^2 n_q{}^2 \qquad (3.6)$$

In the scalar approximation, the boundary conditions require continuity of R and the derivative of R at each interface. In the interface of p^{th} and $(p+1)^{th}$ layer we match the boundary conditions and get a relationship between the coefficient of $(p+1)^{th}$ layer, (A_{p+1}, B_{p+1}) and the coefficients of preceding layers (A_p, B_p) in a form of 2x2 matrix. The relationship is given by:

$$\begin{bmatrix} A_{p+1} \\ B_{p+1} \end{bmatrix} = \begin{bmatrix} a_p & b_p \\ c_p & d_p \end{bmatrix}\begin{bmatrix} A_p \\ B_p \end{bmatrix} \qquad (3.7)$$

Where a_p b_p c_p d_p can be obtained easily which requires multiplication of two 2 × 2 matrix involving Bessel and modified Bessel function. For an initial value of β, using the above 2×2 matrices, one can relate A_N and B_N in term of A_1 and B_1 where the region N is the innermost layer and the region 1 is the outermost region.

$$\begin{bmatrix} A_N \\ B_N \end{bmatrix} = \begin{bmatrix} S_{11} & S_{12} \\ S_{21} & S_{22} \end{bmatrix} \begin{bmatrix} A_1 \\ B_1 \end{bmatrix} \tag{3.8}$$

Where S_{11}, S_{12} etc are the elements of transfer matrix which is the product of various 2x2 matrices of type discussed above.

3.3 Determination of Propagation Constant

For the guided mode the effective refractive must lie between the maximum and the minimum values of refractive index. Since the field is finite at $r = 0$ and $r = \infty$, the coefficient of B_1 and B_N must satisfy

$$B_1 = 0, \qquad B_N = 0, \tag{3.9}$$

Applying these two conditions, we get from equation (3.8)

$$\begin{bmatrix} A_N \\ 0 \end{bmatrix} = \begin{bmatrix} S_{11} & S_{12} \\ S_{21} & S_{22} \end{bmatrix} \begin{bmatrix} A_1 \\ 0 \end{bmatrix} \tag{3.10}$$

Which implies $S_{21} = 0$. (3.11)

Equation (10) is an eigen value equation. Hence in this case by scanning $S_{21}(\beta)$ in the β axis the solution of the above equation will be obtained. Multimode fiber will give us a number of zeros, for the above equation whereas single mode fiber will give only one solution. The solutions in β axis are the mode propagation constants.

3.4 Determination of Leakage Loss

If there is a cladding layer having refractive index higher than or equal to the core index, even the fundamental mode becomes leaky. Calculation of this leakage loss is extremely important for these kinds of fibers. For such leaky modes we have $\beta^2 < k_0^2 n_1^2$, where n_1 is the refractive index of the outermost cladding or the core region. Thus the solution of the outermost cladding is given by the equation (3). The equation (9) is a complex eigen value equation. $S_{21}(\beta)$ will not be equal to zero now. The propagation constant β now has two parts, the real part (β_r) and the imaginary part (β_i). For leaky mode, the outermost region should correspond to a purely outgoing wave,

we must choose such a linear combination of $J_0(k.r)$ and $Y_0(k.r)$ such that it represents an outgoing wave. For this we choose

$$A_1 = \mathrm{i}B_1 \tag{3.12}$$

Thus from the equation (7) we have

$$A_N = A_1(S_{11} + \mathrm{i}S_{12}) \tag{3.13}$$

$$B_N = A_1(S_{21} + \mathrm{i}S_{22})$$

Again we have $\beta^2 < k_0^2 n_N^2$, where n_N is the refractive index of the innermost layer and as before we must have

$$B_N(\beta) = 0 \tag{3.14}$$

This is now a complex eigenvalue equation. We can calculate both the real and imaginary parts of the propagation constant. Now we scan $\left|1/B_N(\beta)\right|^2$ along the real β axis and we obtain Lorentzians, the position of the peak gives the real part of the propagation constant of the mode and the full width at half maxima gives the imaginary part of the mode.

Imaginary part of the propagation constant is the measure of the leakage loss. Loss can be determined by the following relationship:

$$\text{Loss (dB/mm)} = 0.868589 \times 10^{4} \times \text{HWHM} \qquad (3.15)$$

where the dimension of HWHM is μm^{-1}

Equation was solved and the Lorentzian was obtained by simple numerical technique. A program was formed using MATLAB and the values of propagation constant and the leakage loss were obtained. The filed plots were also made by programs MATLAB programs. The flow chart of the program is given below:

3.5 The Flow Chart

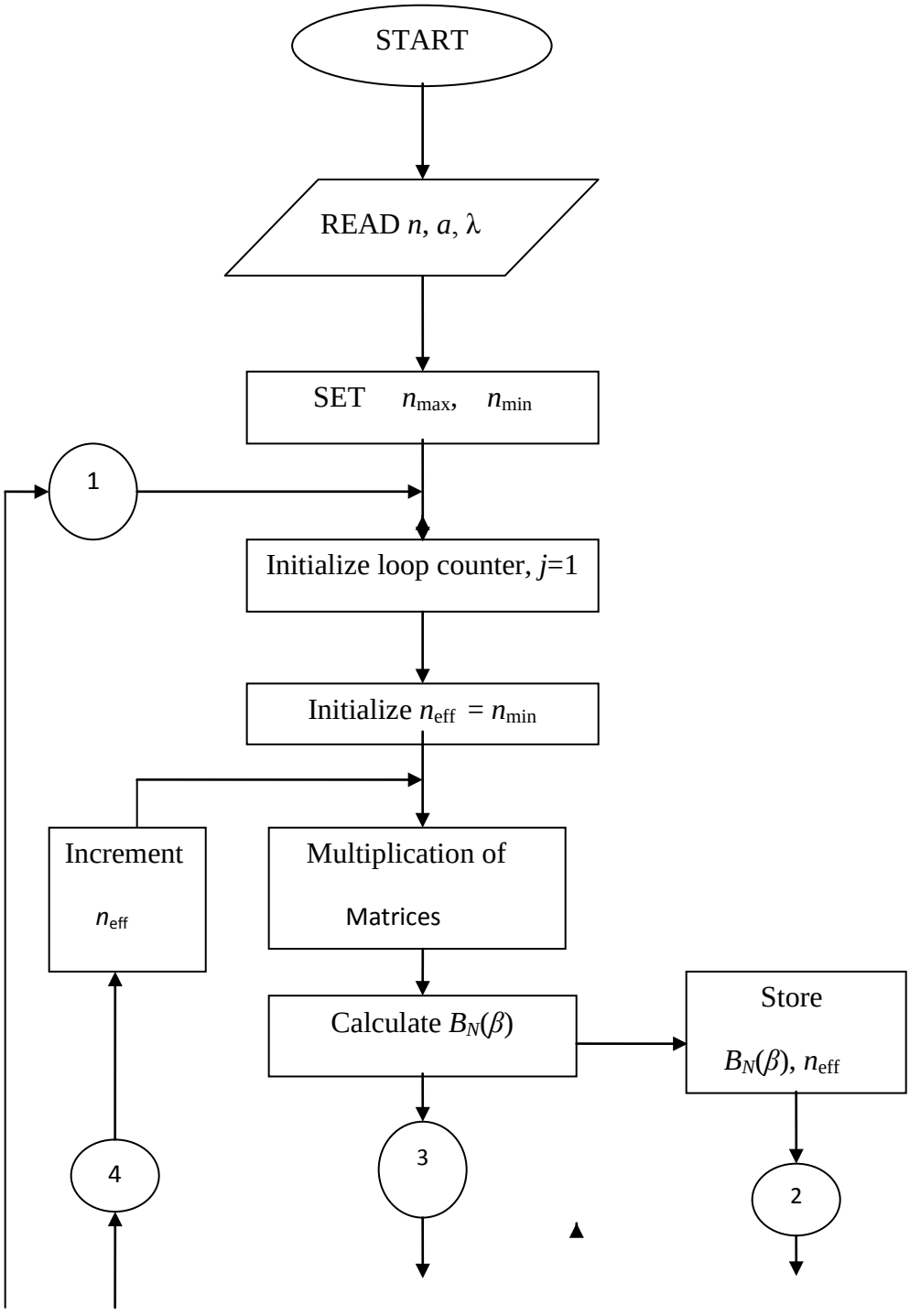

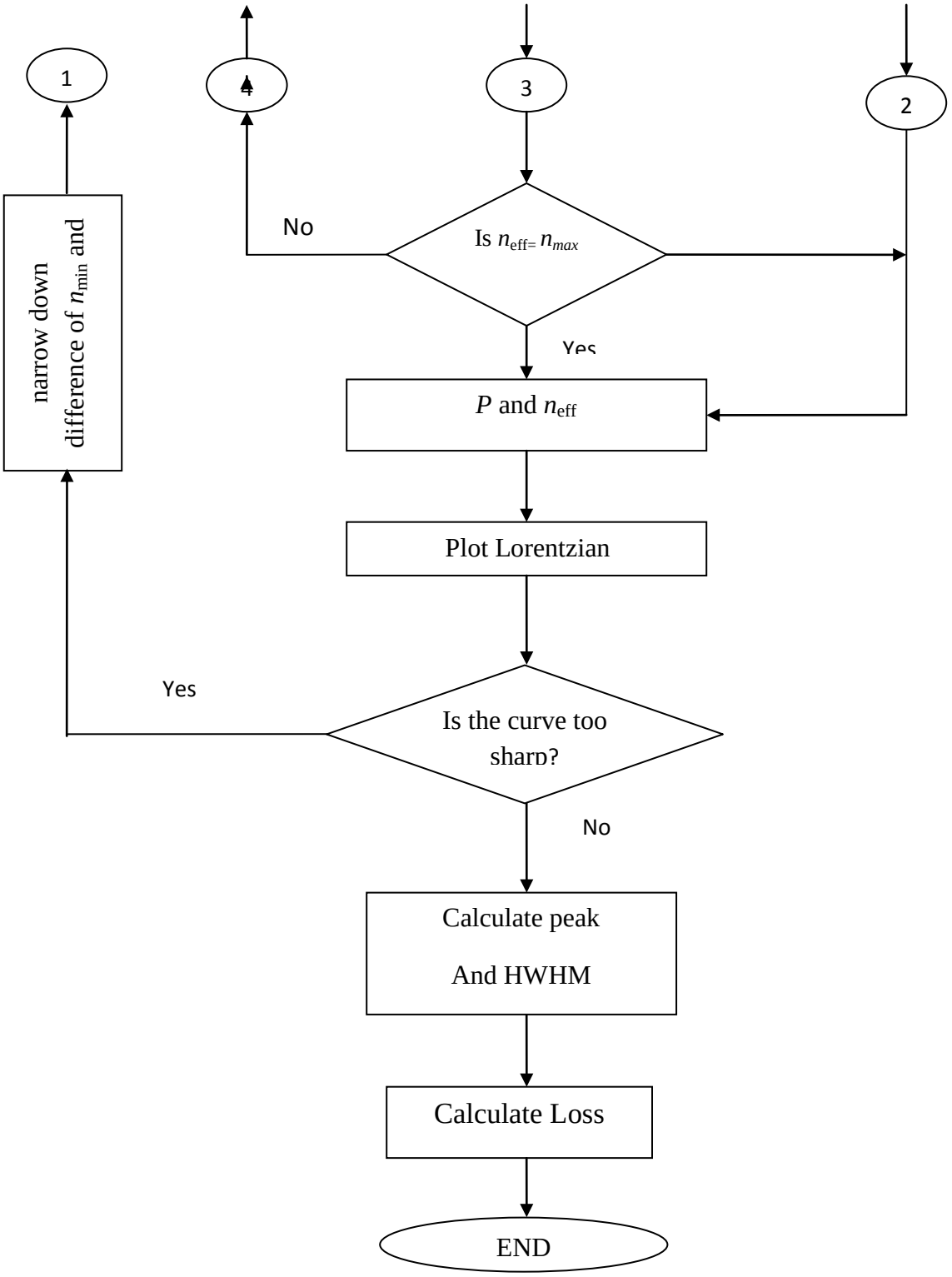
1
4
3
2
narrow down difference of n_{min} and
No
Is $n_{eff=}$ n_{max}
Yes
P and n_{eff}
Plot Lorentzian
Yes
Is the curve too sharp?
No
Calculate peak
And HWHM
Calculate Loss
END

3.6 Basic Principle of Sensing

The basic principle of sensing is to have a mismatch between the diameter of core of uncladded region (sensing region) and core of cladded region. So the whole light from the cladded region does not couple with uncladded region, i.e, some portion of light radiate out when it goes from the cladded region to the sensing region. Hence the modal field is modulated in the sensing region. Hence total power at output is also modulated and become sensitive to the refractive index of the external medium. By measuring the output power and input power we can find out the refractive index of the external medium.

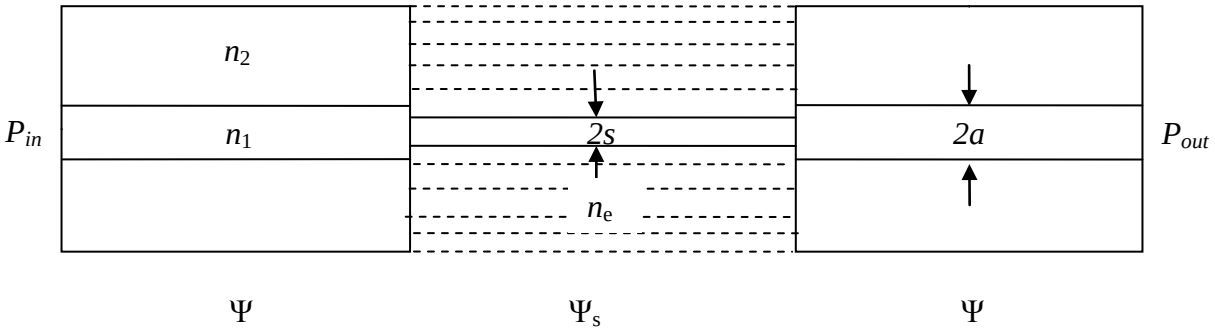

Fig 3.4 Schematic diagram for the core diameter mismatch sensor

Schematic of core diameter mismatch sensor is shown in Fig. 3.4. n_1, n_2, n_{ex} are refractive indices of core, cladding and external medium. Here '*a*' and '*s*' defines the core radii in cladded and sensing region respectively. The modal fields in the cldded and the sensing regions are represented by Ψ and Ψ_s respectively.

If the sensing region of the fiber is placed into a medium having refractive index different from that of cladding, the modal field distribution changes. The overlap of modal fields in cladded region and sensing region gives estimate of fractional power transfer from the input end to output end.

The fractional power transfer is given by

$$\frac{\text{Pout}}{\text{Pin}} = \text{T} \tag{3.16}$$

Where

$$T = \frac{|\iint \psi^* \psi_s r dr d\emptyset|^2}{\iint |\psi|^2 r dr d\emptyset \iint |\psi_s|^2 r dr d\varphi} \tag{3.17}$$

When n_{ex} = 1 there is strong confinement of modal field in the core of the sensing region and the overlap between ψ and ψs is small. As the value of n_{ex} increases the field spreads into the sensing region and the overlap increases. This will change the transmitted optical power.

Chapter 4

Result and Discussions

For the fiber structure proposed in Fig. 3.1 and having profile parameter in *eq.* 3.1, following results are obtained which are responsible for single mode operation and large core area refractive index sensor.

We define the inner core of the fiber by the following parameters:

n_1 = 1.444388, Δ = 0.006, a = 15 μm. The wavelength of operation used is 1.55 μm. We choose the outer core width d_2 = 8 μm, and the separation between the two cores is d_1 = 4μm.

The fiber works on the principle of mode filtering. A high differential leakage loss between the fundamental and the higher-order modes with a nominal loss to the fundamental mode ensures effective single-mode (SM) behavior of the fiber. We use the outer cladding parameters n_3 and d_3 to primarily control the leakage losses of the modes. In fig 4.1 the variation of n_3 is shown against leakage loss.

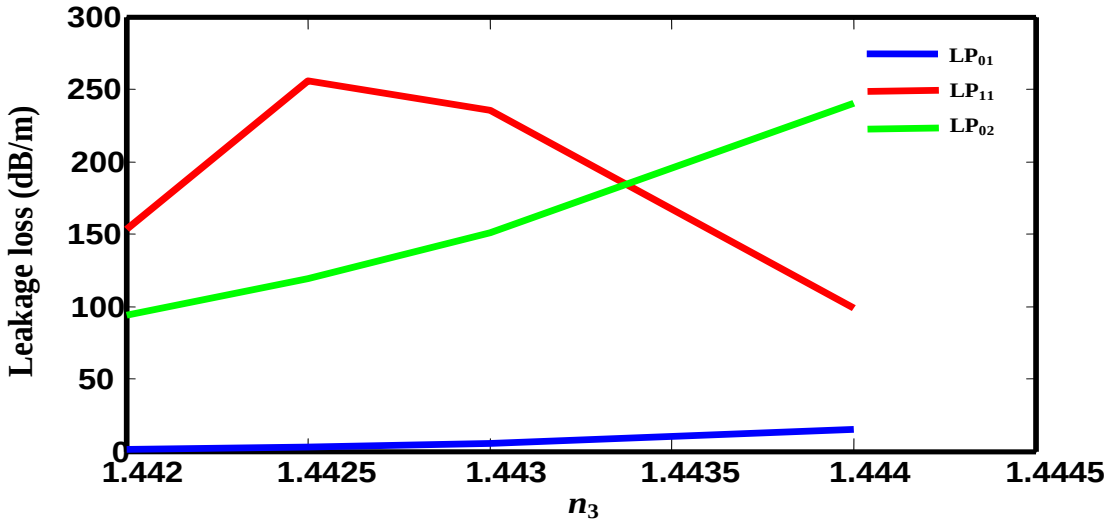

Figure 4.1 Variation of leakage losses of the first three modes of a fiber with outer cladding index n_3.

In Fig. 4.1 the variation of leakage loss with refractive index is shown for first three modes. The leakage losses of the modes increase with the outer cladding index n_3. A peak appearing in the loss curve of the LP_{11} mode around n_3 = 1.4425 reflects the resonant coupling of power from the LP_{11} mode to the outer core, which is highly leaky. Such a coupling of power facilitates the stripping of the LP_{11} mode quickly, even before the LP_{02} mode. At this resonance cladding index it is the differential leakage loss of the LP_{02} mode which now determines the single-mode operation of the fiber. In this way the differential leakage loss between the fundamental and the higher-order modes can be increased significantly, and the minimum propagation length required for stripping off higher-order modes by introducing 20 dB or more loss can be brought down consideration.

The variation of outer cladding width with leakage loss is also studied and shown in the following graph.

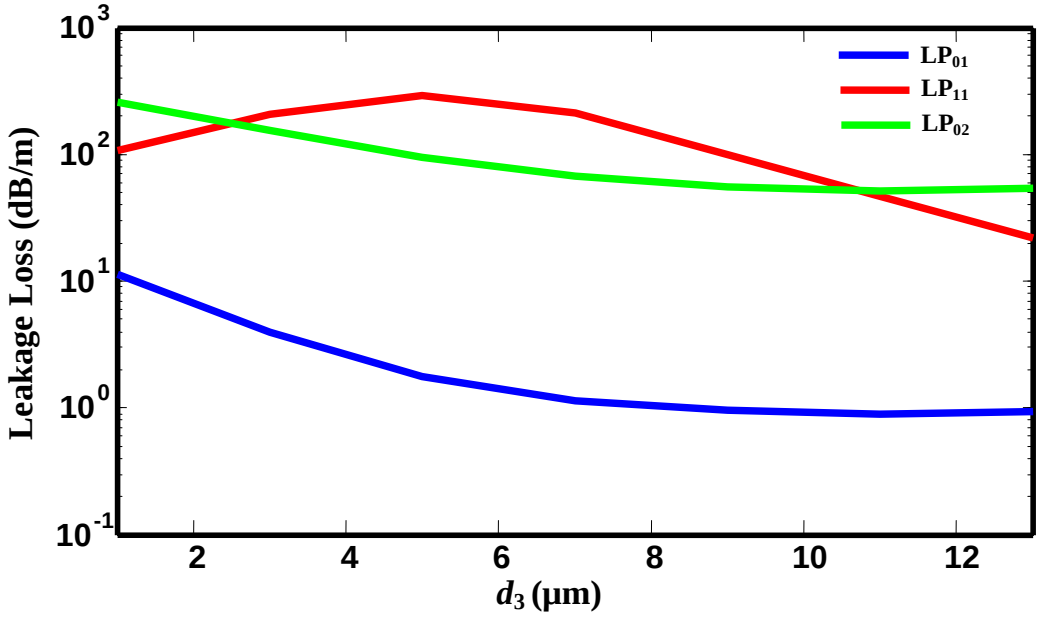

Figure 4.2 Variation of leakage losses of the first three modes with outer cladding width d_3.

The leakage loss of the LP_{01} mode significantly decreases with d_3. For higher-order modes, one can note that in the range 2.4 μm < d_3 < 11.3 μm the leakage loss of the LP_{11} mode surpasses that of the LP_{02} mode and reflects a resonant coupling effect. This range of d_3 can be used to design an large mode area leaky fiber. Figure 4.2 can, thus, help us in choosing

the efficient design parameters. At the first crossing point (d_3 = 2.4 μm) the leakage loss of the LP_{11} and LP_{02} modes is 186 dB m^{-1} and that of the LP_{01} mode is 5 dB m^{-1}. In a design corresponding to this point, the higher-order modes would strip off in just 10 cm propagating distance. However, the fundamental mode would suffer from quite a large loss. When we increase the value of d_3, the differential leakage loss increases, and also the loss of the LP_{01} mode goes down considerably. At the second crossing point (d_3 = 11.3 μm) the leakage loss of the LP_{11} and LP_{02} modes is 55 dB m^{-1} and that of the fundamental mode is 0.04 dB m^{-1}. The higher-order modes, thus, strip off only after 36 cm propagation distance and the fundamental mode suffers from a nominal loss. The fiber, thus, shows an effective SM operation.

To analyze the performance of proposed LMA sensor we have studied the effect of ambient medium on the fractional power output for different etched core radius.

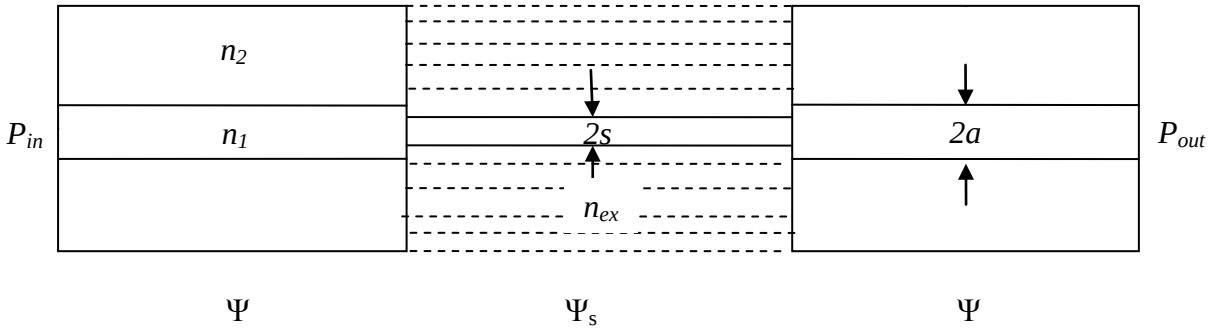

Figure 4.3 Schematic diagram for the core diameter mismatch sensor

In the given schematic n_1, n_2, n_{ex} are refractive indices of core, cladding and external medium. Here '*a*' and '*s*' defines the core radii in cladded and sensing region respectively. The modal fields in the cldded and the sensing regions are represented by Ψ and Ψ_s respectively.

4.1 Same Core Diameter

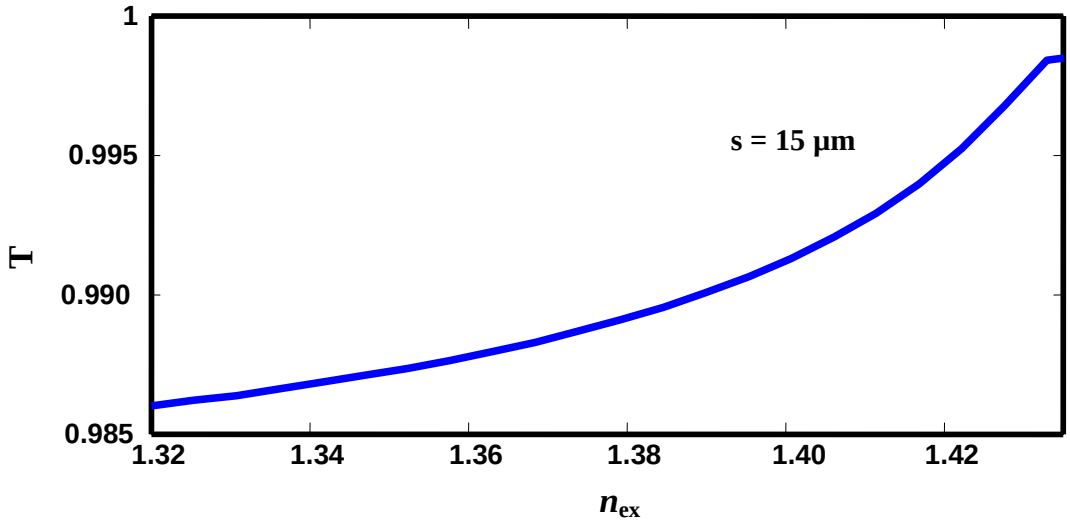

Figure 4.4 Variation of fractional power transfer with the refractive index of the external medium.

The given graph tells us, how the Fractional Power Transfer varies with different External Refractive Index. The total power transfer varies from 98.6% to 99.8% for the variation in external refractive index from 1.32 to 1.44. This shows a small sensitivity for such a large range of refractive index. Hence sensing radius equal to the core radius gives less sensitivity.

The variation of normalized field with radial distance is also shown for in Fig.4.5. It can be seen by the figure that the cladded field and field for external refractive index of 1.44 are almost overlapped to each other. This is due to the approximately 100% power transfer from the cladded region to the sensing region.

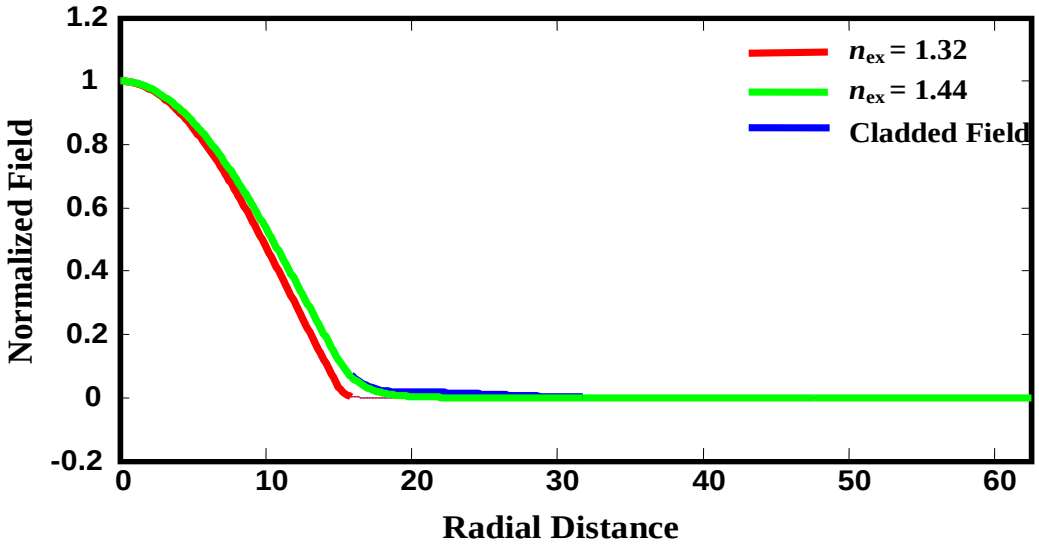

Figure 4.5.Normalized field plot in cladded and sensing region.

4.2 Core Diameter Mismatch

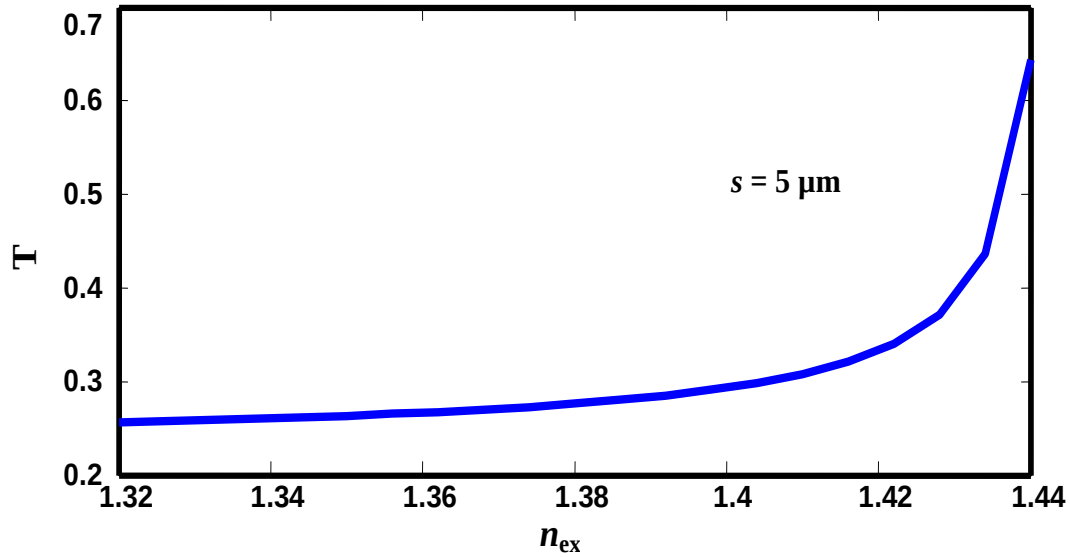

Figure 4.6 Variation of fractional power transfer with the refractive index of the external medium.

Fig. 4.6 shows that the Fractional Power Transfer changes with the change in the Refractive Index of the external medium. As the refractive index of the external medium is increased the overlap integral, i.e, Fractional Power Transfer (T) is also increased. This also shows that the power transfer from the input to the output varies from 25% to 65% as the refractive index of the external medium varies from 1.32 to 1.44. The sensitivity is very high as core diameter mismatch is very high in this case. Such a large variation in the T is due to the fact that filed in the sensing region resembles with the cladded region field on increasing the n_{ex}.

The variation of normalized field distribution with radial distance is also shown below. It can be seen by the graph that field penetration in the cladded region is greater than that in the sensing region as the refractive index contrast is greater in the sensing region.

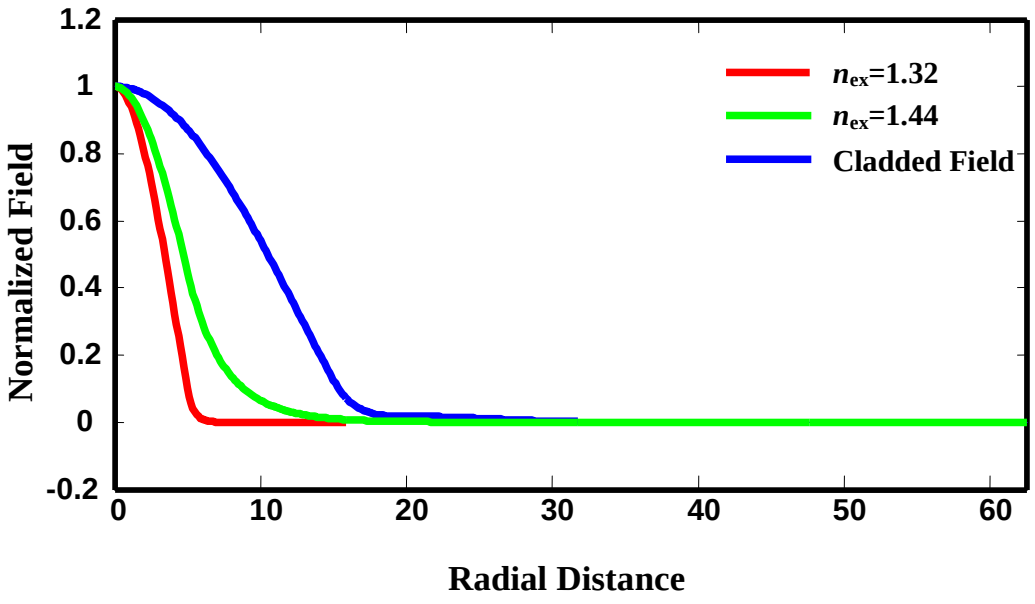

Figure 4.7 Normalized field plot in cladded and sensing region.

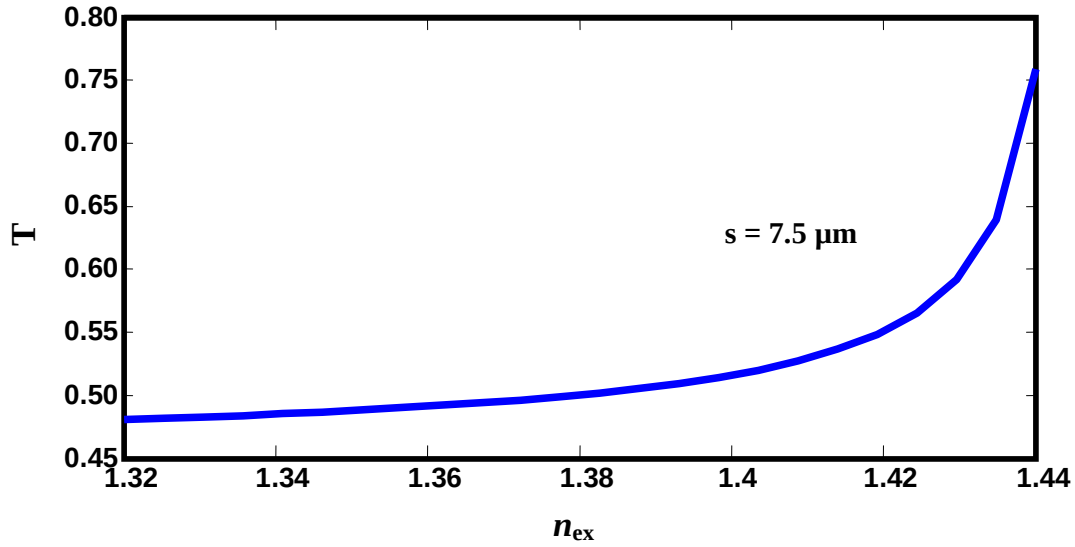

Figure 4.8 Variation of fractional power transfer with the refractive index of the external medium.

This plot gives the variation of Fractional Power Transfer with the External Refractive Index. The power transfer is from 48% to 76% as refractive index varies from 1.32 to 1.44. In this case the power transfer is more than the s = 5 μm case. As the sensing radius is increased more power can propagate.

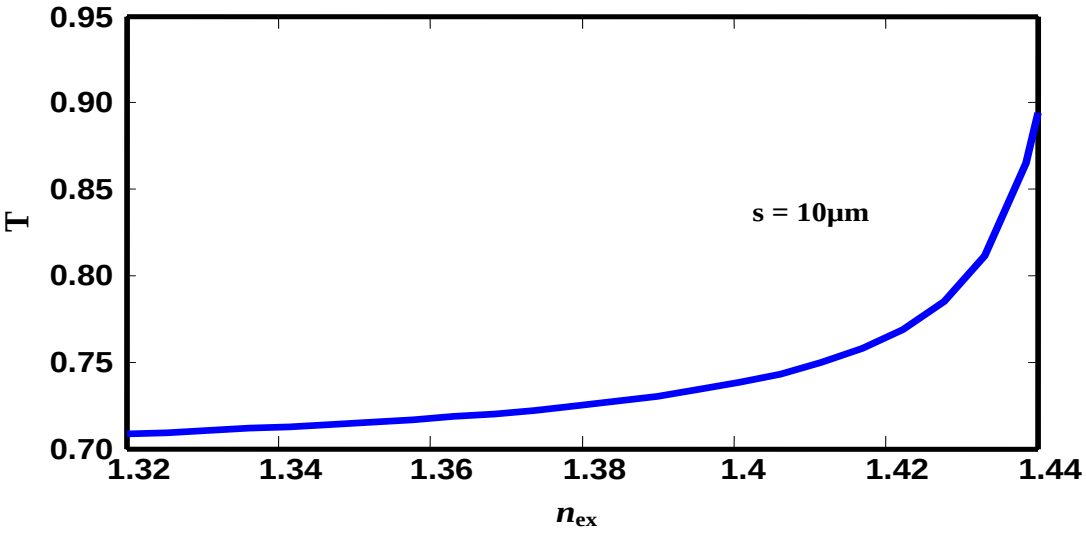

Figure 4.9 Variation of fractional power transfer with the refractive index of the external medium.

Fig. 4.9 shows the variation of Total Power Transfer with External Refractive Index. As the sensing radius is increased the power transfer is also increased. This is due to the fact that large sensing area allows more power to flow into it. The variation of power transfer is from 0.72 to 0.89 for variation in refractive index from 1.32 to 1.44.

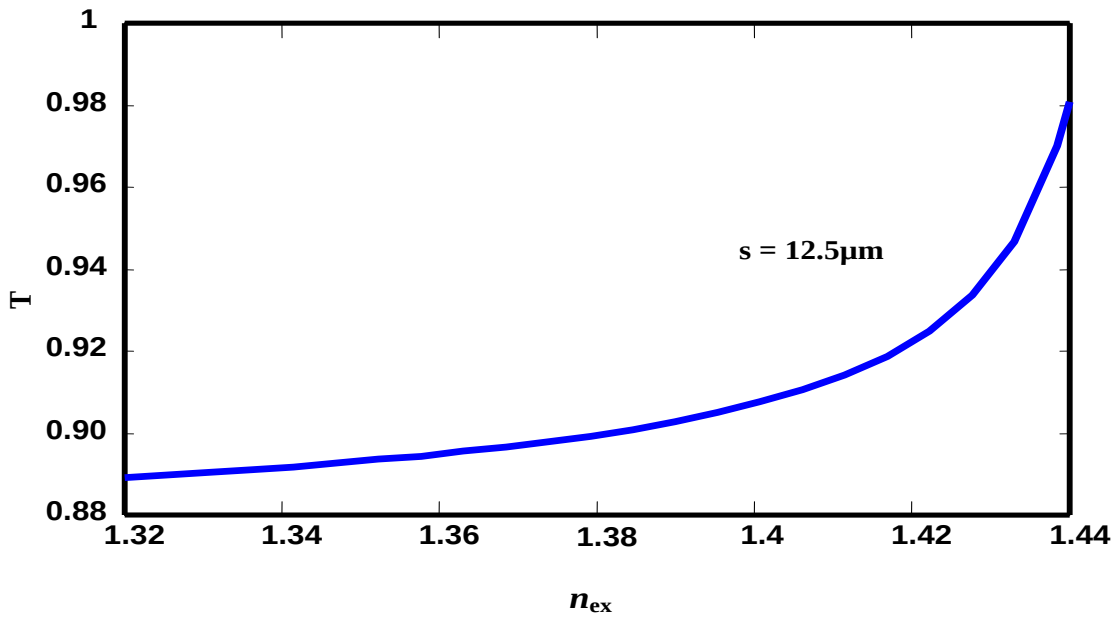

Figure 4.10 Variation of fractional power transfer with the refractive index of the external medium.

The given plot tells us about the variation of total power transfer with external refractive index for the sensing radius of 12.5 μm. The total power transfer varies from 89% to 98% for the variation of refractive index from 1.32 to 1.44.

The total power transfer for the different sensing radius is plotted on the same graph and shown below.

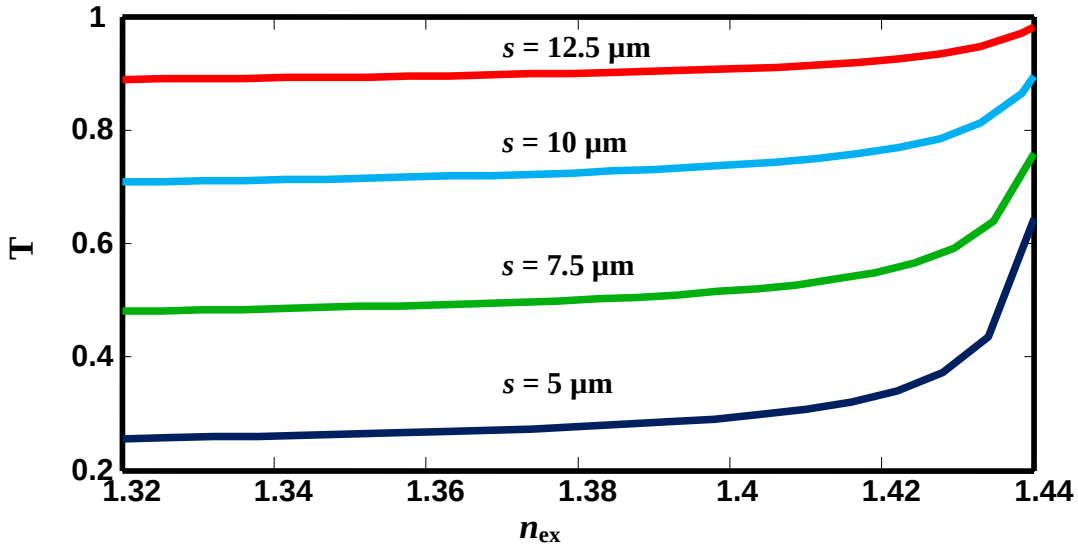

Figure 4.11 Fractional power transfer (T) versus the refractive index of the external medium (n_{ex}) for different sensing radius.

We have plotted T as a function of n_{ex} for different values of s. One can see an improvement in the sensitivity of T with n_{ex}. It can also be seen from the above plot that as core diameter mismatch increases the sensitivity increases. T varies from approximately 25% to 65% for s = 5 μm when n_{ex} is increased from 1.32 to 1.44. In comparison, in single mode optical fiber refractive index sensor configuration of Ref. 10 change is from 50% to 78% for s = 0.7 μm. Again in comparison to the multimode-single-mode-multimode configuration of Ref. 7, change is from 86% to 97% for same s. Hence the above given configuration is far better than given in Ref. 22 and 23. It has good sensitivity for a sensing radius of approximately seven times than the used in Ref. 10 and 7.

We have also calculated the maximum resolution of the proposed sensor. The variation of maximum resolution of designed sensor has also been investigated with sensing radius and shown in Fig. 4.12. For this calculation, we have assumed that T is measured with an accuracy of 1%.

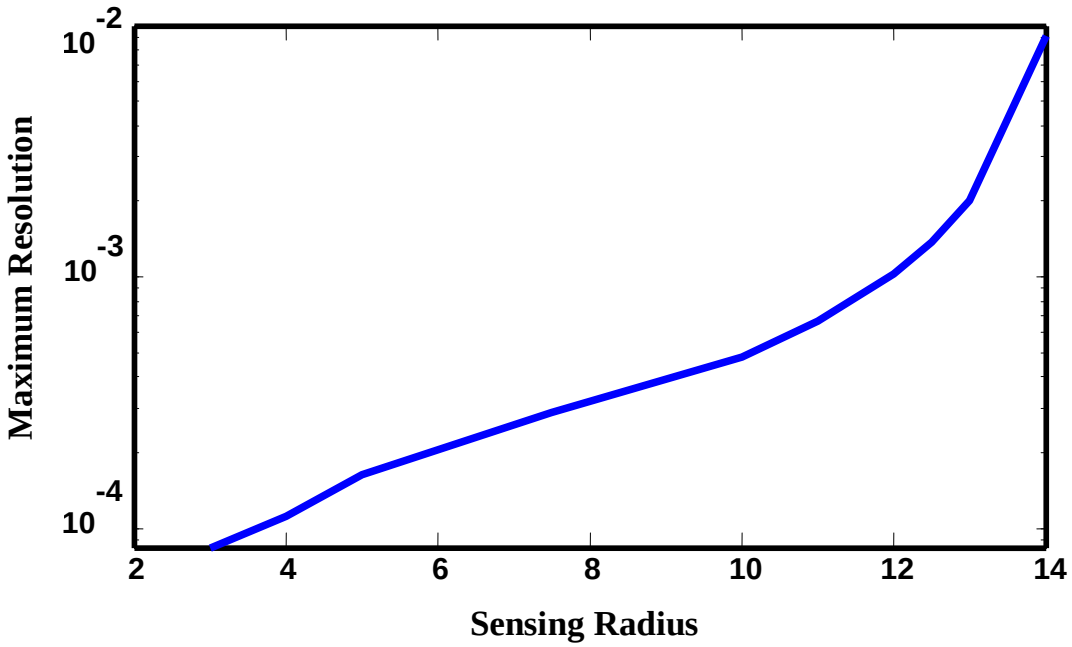

Figure 4.12 Variation of Maximum resolution with sensing radius

From the above graph one can see that maximum resolution of the sensor varies with sensing radius. Due to increase in modal field mismatch, sensitivity of the sensor increases with the decrease in the sensing radius or increase in core diameter mismatch. Sensing resolution decreases from 10^{-4} to 10^{-2} when sensing radius increases from 3 to 14 µm. For the sensing radius of 3μm the maximum resolution is 10^{-4}, however, it makes the devices very difficult for practical applications. We have used the smallest sensing radius 5 μm with a maximum resolution of 1.65×10^{-4} which is almost 6 times better than Ref [10] even with 7 times larger sensing core radius.

Chapter 5

Conclusion and Scope for Future Work

5.1 Conclusion & Scope for future work

A refractive index sensor is proposed with a large core area with a single fiber having effective single mode operation. Single mode operation is made possible with the help of certain design parameters due to which higher order modes are leaked out. Due to large core area it can support large power and is also less fragile. This is a great advantage. Apart from this, T varies from approximately 25% to 65% for s = 5μm when n_{ex} is increased from 1.32 to 1.44. In comparison, in single mode optical fiber refractive index sensor configuration of Ref. 10 change is from 50% to 78% for s = 0.7 μm. Again in comparison to the multimode-single-mode-multimode configuration of Ref. 7, change is from 86% to 97% for same s. The resolution is also estimated for the proposed sensor and found its maximum value to be 8.3×10^{-5} around $n_{ex} = 1.44$. In comparison, in single mode optical fiber refractive index sensor configuration of Ref. 10 maximum resolution is 9×10^{-4} around $n_{ex} = 1.44$. This is also a great advantage over the referenced one.

The results indicate that the core diameter mismatch sensor, in which a part of the core has also been removed, is more sensitive to the same core diameter sensor. Also as we increase the core diameter mismatch the sensitivity also increases. This is due to fact that in core diameter mismatches the overlapping of modal fields between the input region and the sensing region is less due to modal field mismatch which takes place due to both core diameter mismatch and refractive index mismatch. So, the variation of the output power is greater for the case of core diameter mismatch. Hence, the coupling of light between the cladded and sensing region is less for it. Sensitivity increases when the coupling of light between two regions decreases, so the sensitivity is greater for the case of core diameter mismatch.

The proposed sensor can be used as a compact refractometer. It can also be used for other wavelengths for which sensitivity may be more. The fiber parameter can be tuned to design the sensor for desired operating wavelength.

References

1. G. P. Agarwal, 'Fiber-optic communication system', John Wiley & sons.

2. Introduction to fiber optics – A. Ghatak and K. Thyagrajan.

3. Optical fiber Communication- J.M Senior.

4. T. Wei, Y. K. Han, Y.J. Li, H. L. Tsai and H. Xiao, "Temperature-insensitive miniaturized fiber inline Fabry-Perot interferometer for highly sensitive refractive index measurement", Opt. Exp., vol.16, pp. 5764-5769 (2008).

5. R. Jha, J. Villatoro, G. Badenes, and V. Pruneri, "Refractometry based on a photonic crystal fiber interferometer", Opt. Lett., vol.34, pp. 617-619 (2009).

6. W. Liang, Y. Huang, Y. Xu, R. K. Lee, and A. Yariv, "Highly sensitive fiber bragg grating refractive index sensors", Appl. Phys. Lett, vol.86, pp. 122-126 (2005).

7. J. Villatoro and D. Monzoon, "Low-cost optical fiber refractive-index sensor based on core diameter mismatch", J. Lightwave Technol, vol.24, pp. 1409-1411 (2006).

8. K. Thyagarajan, S.Diggavi, A.Taneja, and A. K. Ghatak, "Simple numerical technique for the analysis of cylindrically symmetric refractive-index profile optical fibers", Appl. Opt., vol.30, pp. 3877-3880 (1991).

9. D. B. Stegall and T. Erdogan, "Leaky cladding mode propagation in long period fiber grating devices" IEEE Photon Technol. Lett. vol.11, pp. 343-345 (1999).

10. K. Kamakshi, V. Rastogi, A.Kumar and J.Rai, “Design and Fabrication of a single mode optical fiber based refractive index sensor”, Microwave and optical technology letters, vol.52, pp. 1408-1410 (2010).

11. X. Shu, L.Zhang and I.Bennion, “Sensitivity characteristics of long period fiber gratings”, J Lightwave Technol, vol.20, pp. 255-266 (1999).

12. S. Sandgren, H. Ahlfeldt, B. Sahlgren, R. Stubbe, and G. Edwall “Fiber optical Bragg grating refractometer”, Fiber Integr. Opt., vol.17, pp. 51–62 (1998).

13. T. Takeo and H. Hattori, “Optical fiber sensor for measuring refractive index”, Jpn. J. Appl. Phys., vol.21, pp. 1509–1512 (1982).

14. P. St. J. Russell, “Photonic crystal fibers”, Science, vol.299, pp. 358-360 (2003).

15. J. C. Knight, T. A. Birks, R. F. Cregan, P. St. J. Russell and J. P. De Sandro, “Large mode area photonic crystal fibres”, Electron. Lett., vol.34, pp. 134-141(1998).

16. J. P. Meunier., J. Pigeon and J. N. Massot, “A numerical technique for determination of propagation characteristics of inhomogeneous planar optical waveguide”, Opt. Quantum Electron**.,** vol.15, pp. 77-79 (1983).

17. J. Chilwell and I. Hodgkinson, “Thin films field transfer matrix theory of planner multilayer waveguides and reflection from prism loaded waveguide”, Opt. Society of America vol.1, pp. 742- 749 (1984).

18. N. G. R. Broderick, H. L. Offerhouse, D. J. Richardson, R. A. Sammut, J. Caplen and L. Dong, “Large mode area fibers for high power application”, Opt. Fiber Technol. vol.5, pp. 185-189 (1999).

19. P. Yeh, A.Yariv and E. Marom, “Theory of Bragg fiber”, Optical Society America., vol.68**,** pp. 1196-1198 (1978).

20. H.J. Patrick, A.D. Kersey and F.Bucholtz, “Analysis of the response of long period fiber gratings to external index of refraction”, J Lightwave Technol. vol.16, pp. 1606-1612 (1998).

21. V.Rastogi and K.S. Chiang, “Long period gratings in planar optical waveguides”, Appl. Opt. vol.41, pp. 6351-6355 (2002).

22. D.Monzoon, V.Joel, D.Talavera and D.Luna, “Optical surface Plasmon response sensor with multiple resonance peaks”, Appl. Opt. vol.43, pp. 765-770 (2004).

23. D.Monzoon, J.Villatoro and D.Luna, “Miniature optical refractrometer using cladded multimode tapered tips”, Sens Actuator B Chem. vol.110, pp.36-40 (2005).

24. A.Kumar, V.Rastogi, C.Kakkar and B.Dussardier “Co-axial duel-core leaky fiber for optical amplifiers”, Appl. Opt. vol.10, pp. 1464-1470 (2008).

25. L. G. Cohen, D. Marcus and W. L. Mammuel, “Radiating leaky mode losses in single mode lightguide and depressed index claddings”, IEEE trans. J. Quant. Electron., vol.18, pp. 1467-1471 (1982).

26. P. St. J. Russell, “Photonic crystal fibers”, *Science*, vol.299, p.358 (2003).

27. D. H. Smithgall, T. J. Miller and R. E. Frazee, “A novel MCVD process control technique**”,** IEEE J. Lightwave Tech., vol. 4, pp.1360-1362 (1986).

28. V. Rastogi and K. S. Chiang, “Propagation characteristics of a segmented cladding fiber”, Opt. Lett., vol.26, pp.491-496 (2001).

29. N. A. Mortensen, M. D. Nielsen, J. R. Folkenberg, A. Peterson and H. R. Simonsen, “Improved large mode area endlessly single mode photonic crystal fibers”, Opt. Express., vol.11, pp.456-460 (2002).

30. J. C. Knight, T. A. Birks, R. F. Cregan, P. St. J. Russell and J. P. De Sandro, “Large mode area photonic crystal fibres”, Electron. Lett., vol.34, pp.134-141 (1998).

31. Y. Shizhuo, K. W. Chung, H. Liu, P. Kurtz and K. Reichard, “A new design for non-zero dispersion shifted fiber with a large effective area over 100 μm^2 and low bending and splicing loss”, Opt. Comm., vol.177, pp.225-229 (2000).